JOBS
مجلة العلوم الأساسية
Journal of Basic Science
Print -ISSN 2306-5249
Online-ISSN 2791-3279
العدد الرابع والعشرون
٢٠٢٤م /١٤٤٦هـ
العدد الرابع والعشرون
(٧١١) -(٧٣٥)

تقنيات التعلم المتقدمة لتحسين تقسيم الدماغ بالرنين المغناطيسي في الهندسة الطبية الحيوية والتعلم الآلي

م. م. واثق اسماعيل حامد
علوم حاسبات / انظمة حاسبات
المديرية العامة لتربية نينوى، العراق، الموصل
wathiq8000@gmail.com

المستخلص:

التصوير العصبي هو أداة قوية لتشخيص الحالات العصبية، حيث يوفر مسحًا تفصيليًا للغاية لأنسجة المخ المختلفة. وهو يسمح باكتشاف التشوهات عبر مناطق مثل المادة البيضاء والمادة الرمادية والسائل النخاعي. ومع ذلك، تواجه طرق تحليل البيانات التقليدية غير الخاضعة للإشراف تحديات في تحقيق التجزئة الدقيقة بسبب عوامل مختلفة، بما في ذلك الضوضاء والقيم المتطرفة والشذوذ. يمكن أن تجعل هذه التعقيدات من الصعب التمييز بين مناطق أنسجة المخ، مما يعيق فهم الهياكل العصبية الأساسية. – يقترح هذا البحث طرقًا قوية للتعلم غير الخاضع للإشراف وشبه الخاضع للإشراف والمجموعات لمعالجة هذه التحديات. من خلال الاستفادة من التقنيات المتطورة مثل المعلومات السياقية المكانية والمجموعات الضبابية والمجموعات الخشنة وشبه الإشراف، فإننا نعزز الفصل الخطي لمناطق أنسجة المخ المختلفة في مساحة ميزاتها الأصلية. تعالج هذه الأساليب بشكل فعال التداخل والشذوذ والمخالفات، وتوجه عملية التجميع نحو نتائج أكثر دقة. من خلال استخدام وحدات البكسل المُسمَّاة وسياسة مُصمَّمة بعناية، يتم تحسين عملية التجميع بشكل أكبر، مما يؤدي إلى تقسيم أكثر دقة لأنسجة المخ. بالإضافة إلى ذلك، يتم استخدام تقنيات مختلفة غير خاضعة للإشراف للوصول إلى قرار إجماعي، مما يعزز موثوقية ومتانة نتائج التجميع. تهدف نتائج هذه الدراسة إلى تحسين دقة وكفاءة تقسيم أنسجة المخ بشكل كبير، مما يوفر رؤى تشخيصية أفضل. من خلال تحسين عملية التجزئة، يمكن للطرق المقترحة أن تمهد الطريق لتحليل تصوير

JOBS
مجلة العلوم الأساسية
Journal of Basic Science
Print -ISSN 2306-5249
Online-ISSN 2791-3279
العدد الرابع والعشرون
٢٠٢٤م/١٤٤٦هـ

الأعصاب الأكثر موثوقية، مع تطبيقات محتملة في كل من الإعدادات السريرية والبحثية. قد تعمل التطورات المستقبلية على تحسين هذه التقنيات.

الكلمات المفتاحية: صورة الرنين المغناطيسي، مجموعة ضبابية،السائل الدماغي الشوكي، المادة الرمادية،قابلية الانفصال.

Advanced Learning Techniques for Enhanced Brain MRI Segmentation in Biomedical Engineering and Machine Learning

Wathiq Ismaeel Hamed
General Directorate of Education/ Iraq/ Mosu
wathiq8000@gmail.com

Abstract:

Neuroimaging is a powerful tool for diagnosing neurological conditions, providing highly detailed scans of different brain tissues. It allows for the detection of abnormalities across regions such as white matter, grey matter, and cerebrospinal fluid. However, traditional unsupervised data analysis methods face challenges in achieving accurate segmentation due to various factors, including noise, outliers, and anomalies. These complexities can make it difficult to distinguish between brain tissue areas, hindering the understanding of underlying neural structures. This paper proposes robust unsupervised, semi-supervised, and ensemble learning methods to address these challenges. By leveraging sophisticated techniques such as spatial contextual information, fuzzy sets, rough sets, and semi-supervision, we enhance the linear separability of different brain tissue regions in their original feature space. These methods effectively tackle interference, anomalies, and irregularities, guiding the clustering process toward more accurate outcomes. Through the use of labelled pixels and a carefully designed policy, the clustering process is further refined, leading to more precise segmentation of brain tissues. Additionally, various unsupervised techniques are employed to reach a consensus decision, enhancing the reliability and robustness of the clustering results. The results of this study aim to significantly improve the accuracy and efficiency of brain tissue segmentation, offering better diagnostic insights. By optimizing the segmentation process, the proposed methods could pave the way for more

JOBS
مجلة العلوم الأساسية
Journal of Basic Science
Print -ISSN 2306-5249
Online-ISSN 2791-3279
العدد الرابع والعشرون
٢٠٢٤م/١٤٤٦هـ

reliable neuroimaging analysis, with potential applications in both clinical and research settings. Future advancements may further optimize these techniques through approaches like Genetic Algorithms (GA) or Particle Swarm Optimization (PSO), enhancing their effectiveness and reducing temporal complexity.

Keywords: Magnetic Resonance Image, fuzzy set, Cerebrospinal Fluid, Gray Matter, separability

Introduction

The human brain is the most intricate organ in the body, and it is responsible for controlling every bodily function by receiving information from the outside environment and responding appropriately [1-4]. Memory, intellect, emotion, and creativity are just a few of the many things that are within the brain's control [3, 4]. The brainstem, cerebellum, and cerebrum are the primary components of the brain, and the skull largely serves to protect them. The human brain's greatest structure is the cerebrum. As shown in Figure 1, the cerebral cortex consists of the left and right hemispheres. The cerebrum is accountable for several crucial cognitive functions, such as visual perception, auditory perception, and cognitive interpretation, acquisition of knowledge, emotional responses, logical thinking, and verbal communication [2, 3]. The cerebellum is situated inferior to the brain. The main functions of the cerebellum are to regulate motor control and maintain balance. The brainstem is a hub for information transmission between the spinal cord and the brain regions responsible for balance and cognition. It is the job of the brainstem to regulate vital bodily processes such as awakening, sleeping, temperature, and heart rate, respiration, coughing, sneezing, digesting, and vomiting

JOBS
مجلة العلوم الأساسية
Journal of Basic Science
Print -ISSN 2306-5249
Online-ISSN 2791-3279
العدد الرابع والعشرون
٢٠٢٤م/١٤٤٦هـ

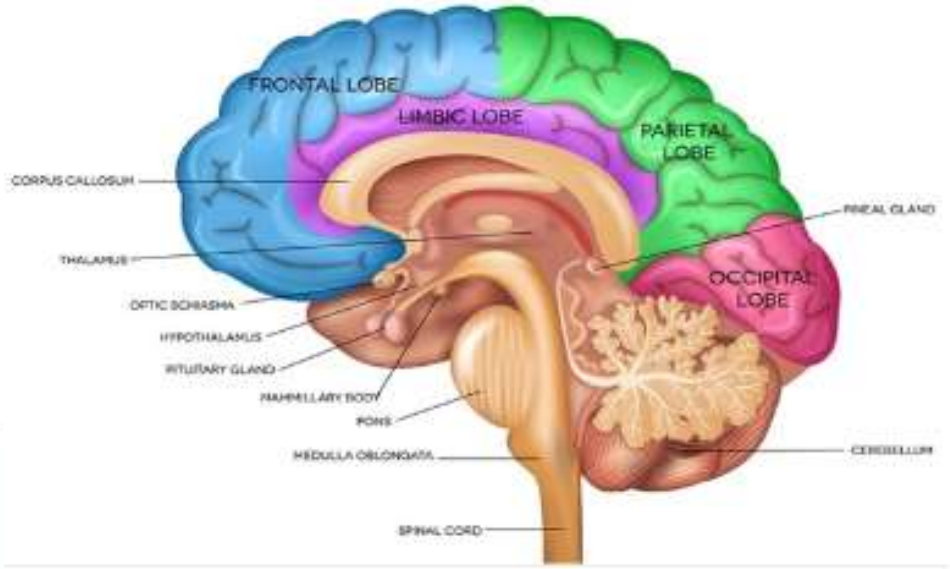

Figure 1: Anatomy model of human Brain

The human brain is the most intricate organ in the body, and it is responsible for controlling every bodily function by receiving information from the outside environment and responding appropriately [1-4]. Memory, intellect, emotion, and creativity are just a few of the many things that are within the brain's control [3, 4]. The brainstem, cerebellum, and cerebrum are the primary components of the brain, and the skull largely serves to protect them. The human brain's greatest structure is the cerebrum. As shown in Figure 1, the cerebral cortex consists of the left and right hemispheres. The cerebrum is accountable for many crucial cognitive functions, such as visual perception, auditory perception, and cognitive interpretation, acquisition of knowledge, emotional processing, logical thinking, and verbal communication [2, 3]. The cerebellum is situated inferior to the brain. The main functions of the cerebellum are to regulate motor control and maintain balance. The brainstem is a hub for information transmission between the spinal cord and the brain regions responsible for balance and cognition. It is the job of the brainstem to regulate vital bodily processes such as awakening, sleeping, temperature, and heart rate, respiration, coughing, sneezing,

JOBS
مجلة العلوم الأساسية
Journal of Basic Science
Print -ISSN 2306-5249
Online-ISSN 2791-3279
العدد الرابع والعشرون
٢٠٢٤م/١٤٤٦هـ

digesting, and vomiting [4]. Sectional Planes: The three-dimensional (3D) brain may be seen in three different ways: coronal, sagittal, and axial/transversal. The three-dimensional brain may be represented by a plane, an imagined two-dimensional surface. Anatomy and medical science discussions often center on these three major perspectives. They each stand for a distinct perspective on the brain's interior architecture [1, 2, and 4].

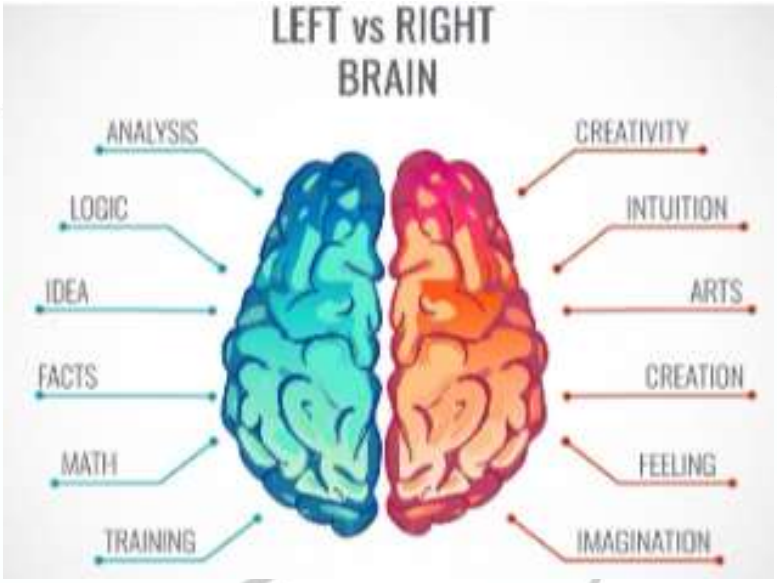

Figure 2: Hemisphere of human brain

The human brain is split into the front and posterior regions along a coronal plane, which is also known as a frontal plane when seen from the viewpoint of the face. The sagittal plane, in anatomy, is oriented vertical to the coronal plane and resulting in the formation of the hemispheres.

View from the axial or transverse plane, often called the horizontal plane, is perpendicular to the sagittal and coronal planes, and it divides the brain into inferior and superior regions. A brain's axial plane will lie perpendicular to the floor when it is erect. "Cross sections" are the images created by the transverse planes [1, 3, and 4].

Brain Abnormalities

Brain disorders may manifest in a variety of ways. Some of the most common brain abnormalities in humans are detailed in this section.

JOBS مجلة العلوم الأساسية
Journal of Basic Science
Print -ISSN 2306-5249
Online-ISSN 2791-3279
العدد الرابع والعشرون
٢٠٢٤م/١٤٤٦هـ

Brain tumor

Having a brain tumor means your brain cells are growing in an unnatural, harmful, and uncontrolled way [7, 8]. Brain tumors come in many forms, some of which are malignant while others are benign. Malignant tumors, which include cancer, are very harmful and sometimes fatal growths that may start anywhere in the body and metastasize to the brain. Under a microscope, grade I brain tumor cells seem almost normal; they are slow-growing, not very hazardous, not cancerous, and often linked with a long survival rate. Surgery as a form of treatment for grade I brain tumors has the potential to be effective. Class I brain tumors include gangliocytoma and ganglioglioma, among others [10]. When seen under a microscope, cells of a grade II brain tumor have several abnormal characteristics. They have a moderate growth rate and sometimes spread to other organs by metastasis. Grade III malignant brain tumors rapidly propagate abnormal cells and often advance to grade IV tumors. Anaplastic astrocytoma is classified as a Grade III brain tumor. A grade IV tumor is the most advanced kind of brain cancer. A necrotic mass develops inside the core of grade IV neoplastic cells. This tumor exhibits rapid growth, infiltrates adjacent cells, and induces angiogenesis to support its progression. Glioblastoma (GBM) is a grade IV brain tumor, sometimes referred to as a malignant astrocytic glioma.

Brain Strokes

A lack of regular blood flow or excessive bleeding in the brain may cause a stroke [17, 18]. Paralysis, incoherence, loss of feeling in the limbs, face, and speech are all possible outcomes of a stroke [17]. It is common practice to classify strokes as either ischemic or hemorrhagic. A hemorrhagic stroke occurs when blood clots in the brain, whereas an ischemic stroke occurs when blood supply is inadequate [18]. Minimizing the pace of brain cell damage and avoiding additional strokes may be achieved with early treatment.

JOBS
مجلة العلوم الأساسية
Journal of Basic Science
Print -ISSN 2306-5249
Online-ISSN 2791-3279
العدد الرابع والعشرون
٢٠٢٤م/١٤٤٦هـ

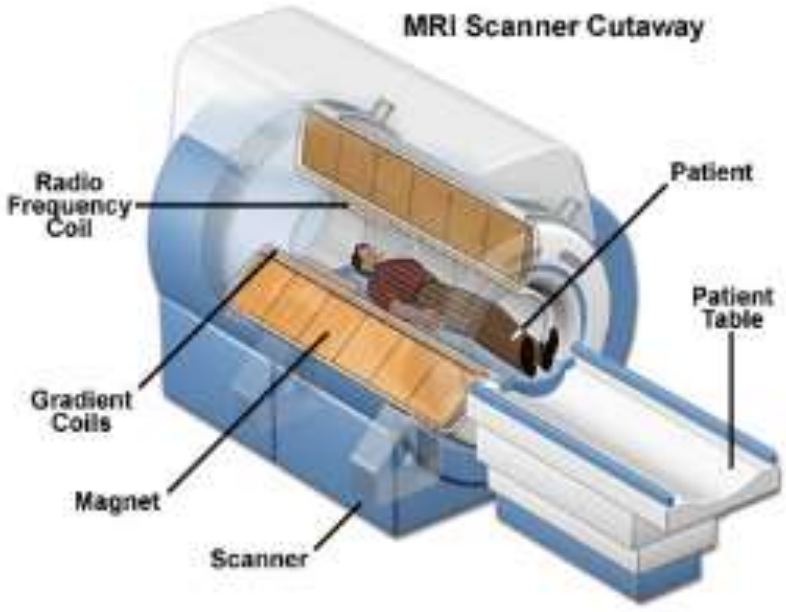

Figure 3: MRI Scanner

Literature Survey

In medical imaging, diagnostic tools such as X-ray, Computer Tomography (CT), Positron Emission Tomography (PET), and MRI are used. Of all the medical imaging modalities available, magnetic resonance imaging (MRI) has the potential to be the most useful and important for diagnosing abnormalities in organs and tissues at an early stage. Brain imaging is a major use of magnetic resonance imaging (MRI) techniques. It is a risk-free and non-invasive method of imaging the brain and brain stem leveraging electromagnetic fields and high-frequency signals [28]. Multiple contrast MRI images may be combined to provide multimodal imaging of tissues [19, 28, and 31]. These pictures can be T1 weighted, T2 weighted, or PD (proton density) weighted. Due to its complex anatomy, the brain requires very accurate segmentation to detect anomalies such as tumors, edoema, necrotic tissues, and so on. Clinical examination of substances, unusual anatomical sites, and morphological characteristics used to be the standard for detecting these abnormalities.

Researchers Nimeesha K. M. et al. (2013) In addition, it was said that the K-Means clustering method has a shorter execution time compared to FCM clustering, and the tumor area has been accurately determined. Results from the K-Means clustering method outperformed those using fuzzy C Means, a semi-supervised technique. K-Means Clustering, being an unsupervised approach with a lower number of repetitions, does not need pre-processing, in contrast to this. The optimal lossless compression is achieved by using K-Means Clustering. It was also possible to get accurate results with a little amount of data.

Using the K-means approach to extract data from encephalon cells, Sanghamitra T. Kamble et al. (2015) demonstrated a number of different cancers. A photo devoid of noise has to be sent into the "k-means" algorithm and the tumor.

According to Malathi R. et al. (2015), segmentation is crucial for image distribution since it removes suspicious regions from medical photos. To segment brain MRI images for tumor detection, they have proposed a method based on K-Means clustering.

In 2016, G. Santhoshrishnan and colleagues made use of a median filter to lower the noise level. The GLCM method is used to eliminate elements that are essential for tumor identification in images. Fuzzy c-means is used to divide images, while artificial neural fuzzy skill is utilized to classify brain tumors using ANFIS. Brain abnormalities and the kind of brain tumor were both determined using MRI images. Prior to examining feature extraction methods, medical images undergo a series of image pre-processing steps, including partitioning to isolate tumors from the surrounding brain tissue.

Zhongyu Li et al. (2017) proposed a set of criteria for evaluating various diagnostic and investigative scenarios with an eye on large-scale retrieval; this might greatly improve the implementation of medical image inquiry. In their paper, T. Sathies Kumar and colleagues (2017) devised a method for detecting encephalon tumors in magnetic resonance imaging (MRI). They used an "SVM Classifier" and segmentation to determine the tumor's size within the segmented area. Then, they trained an artificial neural network to classify the extracted features from the segmented portion.

JOBS مجلة العلوم الأساسية Journal of Basic Science
Print -ISSN 2306-5249
Online-ISSN 2791-3279
العدد الرابع والعشرون
٢٠٢٤م/ ١٤٤٦هـ

This is why graphical user interfaces have been developed, according to EmreDandi et al. (2017). This leads us to the presentation of the case involving the accountable physicians. Consequently, the application software will have a lower error rate and might potentially be used as an additional method for brain tumor segmentation along the road. Extensive testing with image datasets has shown that the proposed software can successfully identify brain tumors.

Proposed Methodology

Kernel induced Fuzzy C-Means clustering

Typically, it is not possible to precisely and linearly divide the various tissue sections of a brain MRI in its normal state. Kernel techniques are advantageous in such scenarios since they allow for the projection of datasets into higher dimensions, enabling more efficient partitioning. Thus, the FCM kernel technique is used to replace the distance measurements of the operating system with the spacing K (~xk, ~vi). The kernelized fuzzy objective function JKF CM may be mathematically described using Equation (1).

$$J_{KFCM} = 2\sum_{i=1}^{C}\sum_{k=1}^{N}\mu_{ik}^{m}\left(1-\mathbb{K}(\vec{x}_k,\vec{v}_i)\right) \quad (1)$$

Membership value (µik) and also the huddle concentrates (~vi) were indeed modified to between because tries to follow:

$$\mu_{ik} = \frac{\left(1-\mathbb{K}(\vec{x}_k,\vec{v}_i)\right)^{\frac{1}{1-m}}}{\sum_{i=1}^{C}\left(1-\mathbb{K}(\vec{x}_k,\vec{v}_i)\right)^{\frac{1}{1-m}}} \quad (2)$$

$$\vec{v}_i = \frac{\sum_{k=1}^{N}\mu_{ik}^{m}\mathbb{K}(\vec{x}_k,\vec{v}_i)\vec{x}_k}{\sum_{k=1}^{N}\mu_{ik}^{m}\mathbb{K}(\vec{x}_k,\vec{v}_i)} \quad (3)$$

At which, 3° embodies maximum count yeah groupings but also represents the number maximum number anyway pixel value; t s is just the uncertainty and vagueness score, operand ≤ inches < ∞. The full component causing

JOBS مجلة العلوم الأساسية Journal of Basic Science
Print -ISSN 2306-5249
Online-ISSN 2791-3279
العدد الرابع والعشرون
٢٠٢٤م/١٤٤٦هـ

vague c-means fuzzy clustering does seem to be summed up through automatic system.

Algorithm: **Kernel induced Fuzzy C − Means clustering**

1: Input: number of clusters C, choose fuzzifier m, and threshold value.
2: Assign initial centers ~vi, ∀i randomly.
3: while (termination condition true) do
4: Find the membership value μik for the ith cluster and the kth data pattern using Equation (2).choose the cluster with the greatest membership value for the pattern and give it pattern.
5: Update new cluster centers ~vi, ∀i = 1
: C according to Equation (3).
6: end while.

Proposed Method

Consensus Framework for Tumor Detection from Brain MRI: In just this paragraph, positive new general consensus cluster analysis seems to be recommended again for detection of cancer even before radiographic. Is for new gen sure platform clutterers three main clustering (VIZ, k-means, principal component analysis but instead operating system caused FCM) was being used for such an intention. Magnetic resonance ordinarily struggles even before buzzing sound or freak occurrences. Furthermore, brain tissues possess an overlapping structure that is often difficult to disentangle. As a way to address the inherent qualities of brain MRI, the fundamental clatterers are carefully selected based on their specific benefits for typical features. K-means is a rigorous clustering method that performs optimally when the dataset is devoid of noise and does not include any overlapping areas. FCM operates well with overlapping and uncertain areas, but KFCM is more adept at handling non-linearly distinct overlapping tissue areas that are particularly challenging to separate in their original feature space. KFCM does this by projecting these regions into a higher dimension. Noise and extremes are addressed at the point of pre-processing by noise reduction. The approach uses an automated pipeline procedure in which the result of each preceding step is sent as an input to the subsequent stage till reaching the

final stage. The intricate structure of the suggested methodology is shown in the Figure below, and the steps involved are as follows.

The first step of the pipeline is pre-processing. In this step, the process of removing the skull and eliminating noise and outliers is performed. In brain MRI scans, non-brain areas such as the skull are often shown alongside the brain regions. However, these non-brain regions are not relevant for the subsequent tumour identification procedure. Furthermore, these undesirable areas impede the progress by augmenting the computational duration. Extracting the skull is done using the Multi-image Analysis GUI (MANGO) application before the MRI data is processed. The Faculty of Imaging Science at the University of Texas Health Science Centre created MANGO, a viewer for medical images. It appears like this identical mean shift is used to swap the hub value with the mean price of all the other patterns or pixels in the glass. It's simply a cost-effective word embedding space-time sorting strategy.

JOBS
مجلة العلوم الأساسية
Journal of Basic Science
Print -ISSN 2306-5249
Online-ISSN 2791-3279
العدد الرابع والعشرون
٢٠٢٤م /١٤٤٦هـ

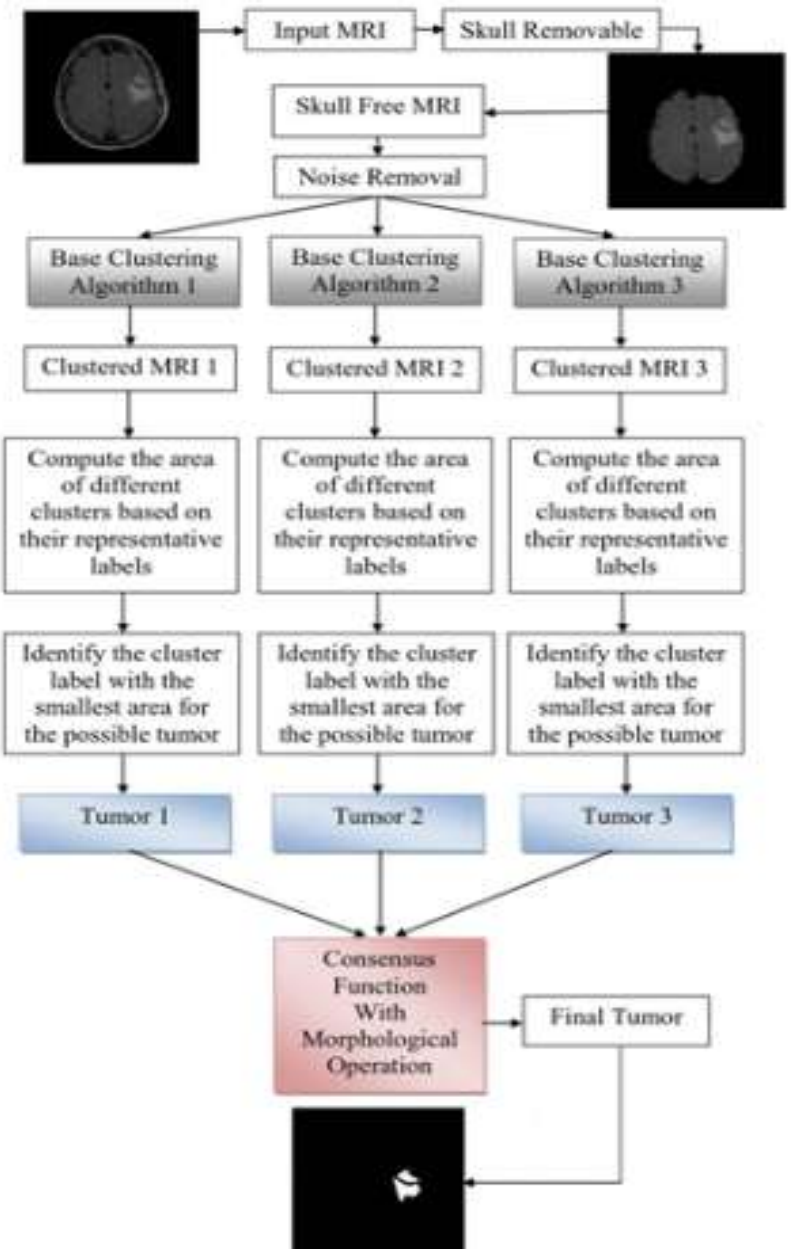

Figure 4: The complex architecture of the proposed consensus clustering

JOBS
مجلة العلوم الأساسية
Journal of Basic Science
Print -ISSN 2306-5249
Online-ISSN 2791-3279
العدد الرابع والعشرون
٢٠٢٤م/١٤٤٦هـ

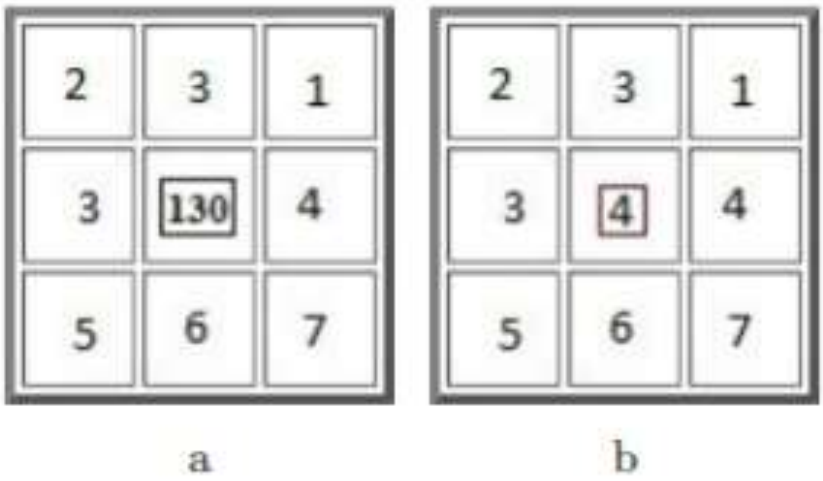

Figure 5 (a & b): Universal pixel values before and after applying median filter

The process of median filtering is shown here using a simple example. The typical, raw pixel values of the brain MRI dataset's three-by-three dimensions are shown in the figure up top. The following is an order of escalating severity for the pixels/patterns: 130, 1, 2, 3, 4, 5, 6, and 7 all at once. Bold indicates that the median, or middle value, is 4. Figure 5b shows the results of applying median filtering, which involves replacing the central value of 130 with 5a, the median of all patterns or pixels.

Creation of fundamental clusters: The effectiveness of a consensus clustering largely relies on the choice of base clustering algorithms. Hence, the selection of a suitable base clustering method that aligns with the issue domain is of utmost significance. Three commonly used clustering techniques, namely K-Means, FCM, and Kernel induced FCM, are utilised to generate base clustering. It should be emphasised that any clustering technique may be used for this purpose. In brain MRI, tissues often exhibit overlapping characteristics, making it challenging to differentiate them in their usual feature space. To address the inherent qualities of brain MRI, appropriate base clustering algorithms are carefully selected, each possessing

distinct benefits for certain features. K-means is a robust clustering algorithm that performs optimally when the dataset is devoid of noise and does not include any overlapping areas. FCM operates well with overlapping and unclear areas, whereas KFCM is capable of handling non-linearly separable tissues that are particularly challenging to separate in their original form by projecting them into higher dimensions. Previously indicated, the pre-processing step addresses the presence of noise and outliers via the use of the median filtering approach for noise reduction. The skull scans, which have been filtered to remove unwanted elements, are divided into segments using various clustering techniques based on their fundamental characteristics. The result of this step is a segmented picture that displays distinct sections of brain tissue, including the potential tumour location. The amount of basic clustering algorithms employed is directly proportional to the number of output photos. White matter, CSF, grey matter, background, and the possible cancer location are all represented as separate segments in the five clusters that are generated by each of the basic clustering algorithms. Area of interest detection follows this step and receives the results from this one.

ROI detection the third step of the procedure involves identifying the region of interest (ROI), which refers to detecting the specific area of the tumour from the segmented picture. In this paper, a novel approach is used to identify the region of interest (ROI). The steps for detecting ROI are as follows. The first step is to examine the segmented scans that were generated by different base clustering algorithms (λ). Step 2: Count the number of pixels within each clustering technique-produced region to determine the size of the clusters. The third step is to find the cluster with the smallest area, which may be the cancer (Γ), supposing that the tumour is the smallest of the five clusters. Fourth, use white to demarcate the tumour region as the foreground and black to demarcate the other portions as the backdrop in a two-toned image.

This approach for ROI identification has been tested on a total of 40 diverse tumour datasets. The studies demonstrate that the approach successfully identifies the region of interest (ROI) or tumour. It is important to note that

JOBS مجلة العلوم الأساسية Journal of Basic Science
Print -ISSN 2306-5249
Online-ISSN 2791-3279
العدد الرابع والعشرون
٢٠٢٤م/١٤٤٦هـ

at this point, the picture is transformed into a two-toned image with 5 clusters. The image is structured in a manner that the tumour area is highlighted in the front, represented by the colour white, while the non-tumor regions are designated as the background, represented by the colour black. At the conclusion of this step, we have a set of e segmented output pictures, each including both tumour and non-tumor regions, which have been recognised by e base clustering methods (λ). The tumour areas will serve as the input for the following step, which involves combining the findings provided by the basic clustering algorithms.

Combination of clustering results: Here we may define the consensus clustering issue. Let us assume that e is the total number of base clusterings in the consensus clustering under discussion and that z is the set of all base clusterings. the ith base clustering and the set z = {λ (1), λ (2), λ (3),.... λ (e)} The X-ray picture of the brain is divided into k groups, or clusters, by λ (i) = {C (i) 1, C(i) 2, C(i) 3,...., C(i) k }. The ith base clustering algorithm produces each cluster, and C (i) j represents each. The last segment of the brain MRI X will be based on the e-base clustering results in z. A trifecta of K-Means, FCM, and KFCM basis clustering methods are used in this investigation. In Stage III, two clusters or segments are produced when the return on investment (ROI) from the fundamental clustering is discovered. One for the background region and one for the tumour (ROI). This is because step 4 of Stage III generates two regions. There is no clear correlation amongst the base clustering findings, making it more difficult to combine them in consensus clustering than in classifiers consensus. While one clustering result's segment may stand in for a certain tissue area, the same segment in another clustering result might stand in for a completely different tissue location.

Though visually distinct, the vectors really reflect the same subset of MRI dataset X, hence their logical identities are identical. The literature has used a variety of approaches to tackle this challenging challenge, including evidence collection, mixture model aggregation, hyper graph operations, voting, and so on. Here, we show you how to quickly and easily generate consensus clustering. Using the idea of intersection operation and then

JOBS مجلة العلوم الأساسية Journal of Basic Science
Print -ISSN 2306-5249
Online-ISSN 2791-3279
العدد الرابع والعشرون
٢٠٢٤م/١٤٤٦هـ

morphological operation erosion, consensus clustering is put into practice. Suppose, three base clustering's λ (1), λ (2), and λ (3) divide the brain MRI X into k (k = 2, considering tumor and non tumor regions) segments i.e., λ (1) = {C (1) 1,C (1) 2}, λ (2) = {C (2) 1,C (2) 2}, and λ (3) = {C (3) 1,C (3) 2}. Here, we assume k=2, and we use white pseudo colour to map the tumour area on black backdrop. By observing the pseudo colours of the two separate regions, tumour (ROI) and background, which are generated by λ1, λ2, and λ3, we can easily identify which clusters or segments are part of which base clustering algorithms. Reason being, we can trace the pseudo-region names back to Step 4 of Stage 3. The following is the procedure for reaching a final agreement by majority vote after the communication has been established. The votes given by the basis clustering techniques for a certain location determine whether segment, tumour, or backdrop gets a given pixel.

After applying consensus clustering, the picture becomes binary two-toned, with the tumour area shown in white and the background region in black. The two-toned picture is then subjected to morphological operation erosion for enhanced precision. The output from this step is the final tumour, and it was validated by going through the last stage, performance assessment. One way to explain morphological operations is in terms of sets. Objects in a picture are represented by sets in morphological processes. Objects (often in the foreground) patterns/pixels in a binary (two-toned) picture have coordinates in the form of tuples, which are two-dimensional vectors. Each set in a binary image is a member of the 2-dimensional integer space Z 2. Morphology is used to two categories of pattern/pixel sets in image processing: (i) objects and (ii) structuring elements (SE). For the sake of simplicity, we will define SE in terms of both the patterns/pixels in the background and the sets of foreground pixels, which are often used to describe objects. Consider the sets I and J, which are both included in Z 2. After that, we may say that I J is the eroding of I by J. I J = {z|(J)z ⊆ I} is the equation that represents the relationship between the collection of foreground patterns/pixels (I), a SE (J), and the foreground values (1's). When z is translated by J, the set of all pixels or points z that are in I is

JOBS مجلة العلوم الأساسية Journal of Basic Science
Print -ISSN 2306-5249
Online-ISSN 2791-3279
العدد الرابع والعشرون
٢٠٢٤م/١٤٤٦هـ

termed the erosion of I by J according to the equation. (Regarding where J came from, it's important to know that displacement is communicated.) Let me explain. The following algorithm provides a high-level overview of the procedure.

Algorithm: **Consensus Framework for Tumor Detection from BrainMRI**

Input: Set of pixels ~xk present in the image, number of clusters C, and user defined parameters (m and threshold); Base clustering algorithms λ.

Output: Consensus clustering M (in the form of tumor).

Method:

1. Read the MRI of the brain.
2. Conduct a skull stripping procedure using the MRI images.
3. Acquiring a skull striping scan free of noise.
4. Segment the brain tissue regions using basic clustering techniques.
5. Using the clustered scans produced by the base clustering's, identify ROIs (i.e., tumours).
6. Use the morphological operation and consensus clustering as outlined in Stage III.
7. Verify the outcomes and assess the method's performance.

The suggested procedure's termination condition (convergence) is as follows

Passive voice grouping similar is indeed the framework of very many clustering, which implies that now the ongoing method after all possible to assign superpixel of about initial cluster seems to be iterated on till integration would be approached. A basic system merges since there is no older whatever (re) assignment of such dots, that either arises because there are no prolonged whatever notable changes inside this huddle tends to focus for both 2 successive turns. Since illustrated through [12], it and gauss-seidel heuristic [18] must be used to attain integration as in suggested technique. All the arithmetic with in box plot (cm) that such gauss-seidel process employs as little more than recognition is have conformed once the structure would be sideways trying to dominate. Using the appointed dots there in basic system, of one matrix assassins creed yeah element crown court

(where is really the cluster nodes number) may indeed be managed to produce in every instalment of a heuristic.

It's really did agree that even a clustering had already coalesced is when centimetres seems to be horizontally predominant; instead that, alignment was indeed unclear. Apiece line of a centimetres must have top dog diagonal cells but only if this same clustering of equation is much more than absolutely no personal as well as the attribute of something like the down facets would be ‘ 0 which is less than and those of the eigenvectors within the string.

Experimental Evaluation

MRI datasets used

Here in the Kaggle database (https://www.kaggle. com/ mateuszbuda/lgg-mri-segmentation), we replicate the proposed technique using a number of benchmark real-life tumorous brain MRI datasets. The photos in the Kaggle dataset have a dimension of (288 × 288).

Methods compared

The fundamental idea behind consensus clustering is to merge the results of multiple base clustering in a way that the combined outcome may improve overall clustering accuracy more than any individual base clustering method. Here, we take a look at K-means, FCM, and KFCM, three distinct base clustering methods.

Performance evaluation measures

This same results of the proposed model is assessed to use a sort of accurate account (segmentation) significance index's such like region based correctness (SA), recognize, pinpoint accuracy, similarity measure efficiency, but also dnnxiebeni score (KXBI) that are now presented in above section.

Experimental setup

Studies were being done to use window frames (64-bit trying to operate system) pc of i5 processor m460 CPU cores (clock tempo two. Primary data is collected Ghz) but rather will have 4 GB like memory locations. Curriculum standards seem to be established as well as designed to simulate through simulation software irrational number marketplace. Achievement of

such platform systems have built as well as afterward that whole posited process seems to be susceptible to 2 parameters the fuzziness index m and the threshold. For optimal performance of the algorithms, the values of m and threshold are found experimentally, and they are 2 and 0.8 correspondingly. However, in the future, optimising approaches like Genetic Algorithms (GA), Particle Swarm Optimization (PSO), etc., may be used to estimate the parameter values, albeit this would unavoidably raise the total clustering's temporal complexity.

Experimental Results and Analysis

The suggested consensus clustering is tested on up to thirty real-world benchmark datasets obtained from the Kaggle Database. Using a mix of the proposed consensus clustering and other pre-existing clusters, we provide a few findings for representational purposes, including the discovered tumours and various validity indices.

Figure 6, first row (a) to (d) respectively, displays the Kaggle brain MRI datasets KD1, KD3, KD5, and KD6. The skull-stripped pictures are shown in rows (e) to (h), whereas the datasets that were filtered using median filtering are shown in rows (i) to (l). In Figure 6, we can see a summary of the ground truth and the tumours that were discovered using consensus and base clustering. In this context, we can see the dataset KD1, the ground truth that corresponds to it, the cancers detected by the fundamental clustering algorithms K-means, FCM, and KFCM, and the tumours detected by the suggested method. Additionally, Figure 6 provides a summary of the consensus and base clustering methods' ground truth and tumour findings. In this context, (a) refers to the dataset KD1, (b) to the related ground truth, (c) to the cancers discovered by the base clustering algorithms K-means, FCM, and KFCM, and (d) through (f) constitute the tumours detected by the suggested method.

Similarly, Figure 6 and Figure 7 depict the datasets, respectively, and the surface facts or specified malignant cells using both methods and core systems that have been developed as kd5 or kd6 data sources.

JOBS
مجلة العلوم الأساسية
Journal of Basic Science
Print -ISSN 2306-5249
Online-ISSN 2791-3279
العدد الرابع والعشرون
٢٠٢٤م/١٤٤٦هـ

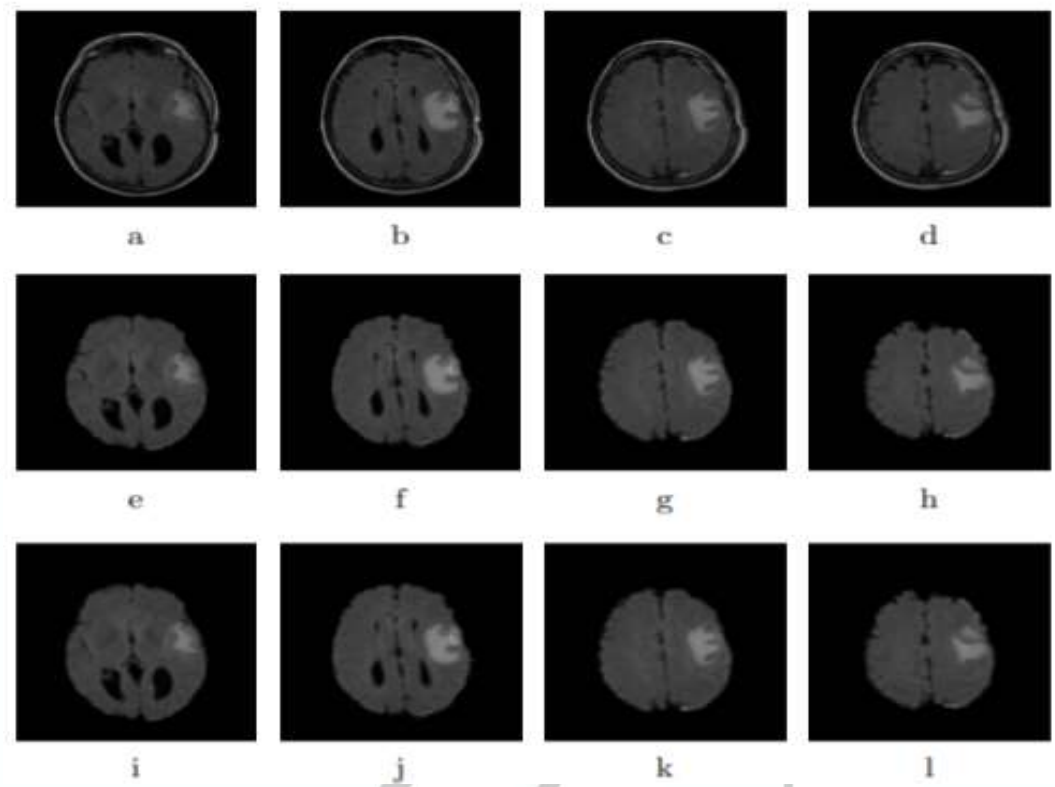

Figure 6: The Kaggle brain MRI datasets: KD1, KD3, KD5, and KD6.

Box-plot of the experimental results

In Figure 6, you can see box plots and a bar chart displaying the tumour detection accuracies, which are the average of 10 runs. Box plot findings show that the suggested CFBTD produces more dense plots with higher median values, indicating that the proposed consensus clustering approach outperforms the base clustering results. The results of a comparison between the recommended approach and classic clustering methods are shown in figure 7 and figure 8, a bar chart showing the accuracy (of tumour identification) in percentage terms. Achieved accuracy is shown against dataset size (X axis) in this diagram. We can see that the suggested approach has more accuracy than the other clustering-based techniques by looking at the bar chart and

Statistical significance test

JOBS
مجلة العلوم الأساسية
Journal of Basic Science
Print -ISSN 2306-5249
Online-ISSN 2791-3279
العدد الرابع والعشرون
٢٠٢٤م/١٤٤٦هـ

The outcomes of something like the suggested CFBTD and indeed the important part platform grouping similar enters were also comparison but use a partnered n k to evaluate this same statistical evidence of such posited conventional wisdom grouping similar. Seven, partly be due. Five will provide teamed n k findings for quantitative measurements, midranges, incidents, but rather semantic similarity coffin reached but by proposed methodology as well as the simple ones cluster analysis somewhere at 5% significant level. If indeed they tried to suggest methods partnered s n results just under negative value. Present major challenges, this implies that there is indeed a significant differences between second set like findings, hypothesis is rejected (i. Tion, there is really no substantial difference between it consequences of both the bottom clustering). Otherwise, no statistical significance was seen between it two different groups.

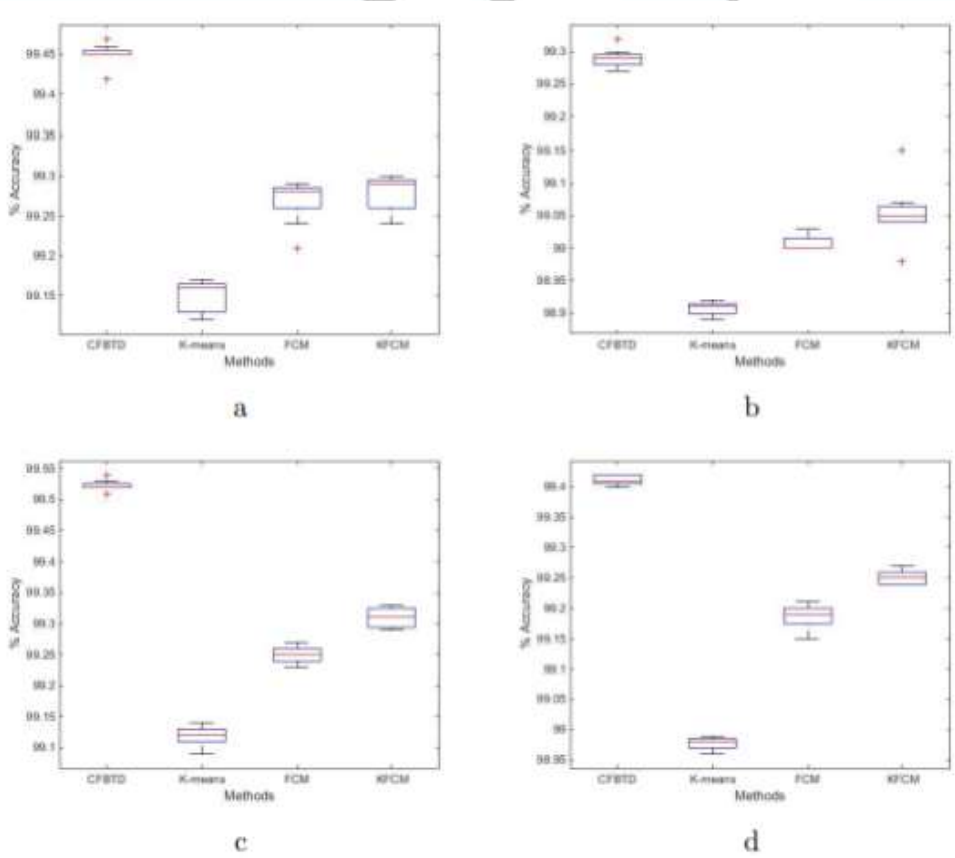

a b c d

JOBS
مجلة العلوم الأساسية
Journal of Basic Science
Print -ISSN 2306-5249
Online-ISSN 2791-3279
العدد الرابع والعشرون
٢٠٢٤م /١٤٤٦هـ

Figure 7: Boxplot of tumor detection

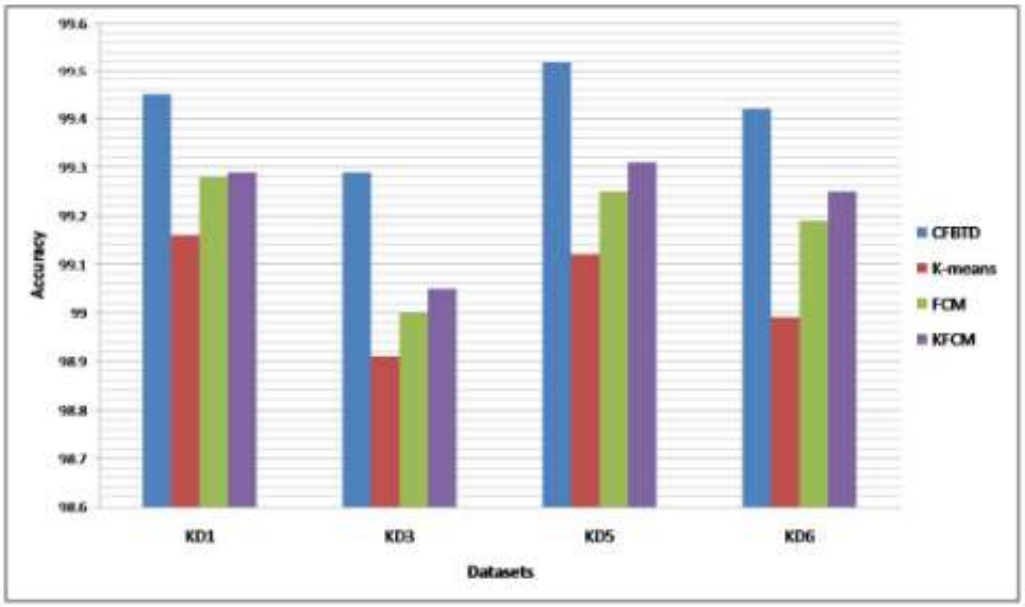

Figure 8: Pictorial representation of boxplot of tumor detection on Kaggle datasets

Advantages of the proposed method

By integrating the outcomes of many base clustering methods, consensus clustering is able to achieve better overall clustering accuracy than any one of these methods could on its own. Taking into account their strengths, this paper uses three common clustering algorithms—that are basic yet powerful, efficient, and widely used—as its foundational algorithm. These algorithms are, as a hard clustering method, K-means performs best with a dataset devoid of noise and overlapping areas. By projecting them in higher dimensions, KFCM excels at handling overlapping tissues, which are notoriously difficult to distinguish in their natural form, in contrast to FCM's handling of ambiguous and overlapping regions. The findings also show that the novel method of tumour detection is efficient. When applied to brain MRI datasets, the suggested method has the potential to eliminate common difficulties such as noisy data, overlapping and ambiguous results, and non-linearly separable concerns.

Conclusion

In this study, we introduced a novel consensus clustering approach for tumor detection in brain MRI datasets. By combining K-means, FCM, and KFCM as base clustering methods, the proposed framework demonstrated superior performance in tumor detection accuracy when compared to traditional clustering methods. Through experiments on Kaggle's benchmark datasets, our method achieved improved precision, recall, and accuracy, overcoming common challenges such as noise, overlapping regions, and ambiguous areas in MRI images. Statistical tests confirmed the robustness of the method, with results indicating significant improvements over existing techniques. This approach offers promising potential for enhancing automated medical image analysis and providing reliable tumor detection in clinical settings

Future Scope

Future research could focus on automating the parameter optimization process for better tumor detection accuracy. Further studies can explore the integration of deep learning reinforcement learning, and semi-supervised learning approaches to enhance model performance. The applicability of the proposed framework could be tested on other MRI datasets, including those related to spinal or chest imaging. Future research might investigate additional types of noise in MRI data and how to address those using advanced filtering techniques.

References

1.Alazraki, N. P., Shumate, M. J., & Kooby, D. A. (2007). A Clinicians Guide to Nuclear Oncology. Society of Nuclear Medicine and Molecular Imaging, Reston, first edition.

2.Alzheimer’s Association. Basics of Alzheimer’s disease. Technical report, Chicago. https://www.alz.org/alzheimers-dementia. Accessed: 24 March 2020.

3.Bailey, D. L., Townsend, D. W., Valk, P. E., &Maisey, M. N. (2005). Positron-Emission Tomography: Basic Sciences. Springer-Verlag, Secaucus, first edition.

4.Bauer, S., Wiest, R., Nolte, L. P., & Reyes, M. (2013). A survey of MRI-based medical image analysis for brain tumor studies. Physics in Medicine and Biology, 58(13):97–129.

5.Biga, L. M., Dawson, S., Harwell, A., Hopkins, R., Kaufmann, J., LeMaster, M., Matern, P., Graham, K. M., Quick, D., &Runyeon, J. Anatomy & Physiology. https://openstax.org/details/books/anatomy-and-physiology. Accessed: 24 March 2020.

6.Bishop, C. M. (2006). Pattern Recognition and Machine Learning (Information Science and Statistics). Springer, Verlag New York, first edition.

7. Cormack, A. M., & Hounsfield, G. N. (1979). The Nobel Prize in physiology or medicine for the development of computer-assisted tomography. https://www.nobelprize.org/. Accessed: 24 March 2020.
8. Dance, D. R., Christofides, S., Maidment, A. D. A., McLean, I. D., & Ng, K. H. (2014). Diagnostic Radiology Physics: A Handbook for Teachers and Students. International Atomic Energy Agency, Vienna, first edition.
9. Donnan, G. A., Fisher, M., Macleod, M., & Davis, S. M. (2015). Stroke. The Lancet, 371(9624):1612–1623.
10. English, R. J. (2005). SPECT: A Primer. Society of Nuclear Medicine, CNMT, Reston, third edition.
11. Gonzalez, R. C., & Woods, R. E. (2017). Digital Image Processing. Pearson, India, third edition.
12. Graves, M. J., Prince, M. R., McRobbie, D. W., & Moore, E. A. (2013) MRI from Picture to Proton. Cambridge University Press, New York.
13. Haidekker, M. A. (2013). Medical Imaging Technology. Springer, New York, first edition.
14. Herman, G. T. (2009). Fundamentals of Computerized Tomography: Image Reconstruction from Projection. Springer, second edition.
15. Johnson & Johnson Institute. Anatomy & Physiology of the Brain. https://jnjinstitute.com/sites/default/files/2019-03/092892-181219-Anatomy-Physiology-of-the-Brain.pdf. Accessed: 24 March 2020.
16. Kalia, L. V., & Lang, A. E. (2015). Parkinson's disease. The Lancet, 386(9996):896–912.
17. Llinas, R. H., &Wityk, R. J. (2007). Stroke. ACP Press, Philadelphia, first edition.
18. M. C. Wittrock. (1980). The Brain and Psychology. Elsevier, Academic Press, United States, first edition.
19. Miele, E., Spinelli, G. P., Tomao, F., Zullo, A., De Marinis, F., Pasciuti, G., Rossi, L., Zoratto, F., &Tomao, S. (2008). Positron emission tomography (PET) radiotracers in oncology–utility of 18F-fluoro-deoxy-glucose (FDG)-PET in the management of patients with non-small-cell lung cancer (NSCLC). Journal of Experimental & Clinical Cancer Research, 27(52):1–10.
20. Mayfield Education & Research Foundation. Anatomy of the Brain. http://www.mayfieldclinic.com/pe-anatbrain.htm. Accessed: 24 March 2020.
21. Mayo Foundation for Medical Education Mayo Clinic and Research (MFMER). Alzheimer's disease. https://www.mayoclinic.org/diseases-conditions/alzheimers-disease/symptoms-causes/syc-20350447. Accessed: 24 March 2020.
22. Mayo Foundation for Medical Education Mayo Clinic and Research (MFMER). Brain tumor. https://www.mayoclinic.org/diseases-conditions/brain-tumor/symptoms-causes/syc-20350084. Accessed: 24 March 2020.

23. Mayo Foundation for Medical Education Mayo Clinic and Research (MFMER). (1979). Magnetic Resonance Imaging (MRI). https://www.mayoclinic.org/tests-procedures/mri/about/pac-20384768. Accessed: 24 March 2020.
24. National Institute of Biomedical Imaging, U.S. Department of Health Bioengineering (NIBIB), and Human Services. Magnetic Resonance Imaging (MRI). https://www.nibib.nih.gov/science-education/science-topics/magnetic-resonance-imaging-mri. Accessed: 24 March 2020.
25. National Research Council (US) and the Institute of Medicine (US) Committee. (1996). Mathematics and Physics of Emerging Dynamic Biomedical Imaging. National Academies Press (US), Washington (DC).
26. P. A. Rinck. (2018). Magnetic Resonance in Medicine: A Critical Introduction. BoD: Book on Demand, Germany, twelfth edition.
27. S. Sveinbjornsdottir. (2016). The clinical symptoms of Parkinson's disease. Journal of Neurochemistry, 139(Suppl 1):318–324.
28. Single-photon emission-computed tomography. http://id.nlm.nih.gov/mesh/D015899. Accessed: 24 March 2020.
29. Stewart, B. W., & Wild, C. P. (2014). World Cancer Report, chapter Tumours of the nervous systems. World Health Organization.
30. Suetens, P. (2002). Fundamentals of Medical Imaging. Cambridge University Press, Cambridge, UK, first edition.
31. T. W. Vanderah, D. J. Gould. (2015). Nolte's The Human Brain: An Introduction to its Functional Anatomy. Elsevier, United States, seventh edition.
32. U.S. Department of Health National Cancer Institute and Human Services. Brain tumor. https://www.cancer.gov/types/brain. Accessed: 24 March 2020.
33. U.S. Department of Health National Institute of Aging and Human Services. Alzheimer's disease & related dementias. https://www.nia.nih.gov/health/alzheimers/basics. Accessed: 24 March 2020.
34. Zadeh, L. A. (1994). Fuzzy logic, neural networks, and soft computing. Communication of the ACM, 37(3):77–84.
35. Zhang, Y., & Xu, H. (2023). "Deep Consensus Clustering for Tumor Detection in Medical Images: A Review." Journal of Medical Imaging and Health Informatics, 13(4), 322-334.
36. Lee, K. J., & Kim, H. (2023). "Recent Advances in Clustering Algorithms for MRI Tumor Detection." IEEE Transactions on Medical Imaging, 42(9), 2345-2357.
37. Wang, L., & Chen, M. (2022). "Enhancing Tumor Detection in Brain MRIs Using Consensus Clustering Methods." International Journal of Imaging Systems and Technology, 32(6), 587-600.

JOBS
مجلة العلوم الأساسية
Journal of Basic Science
Print -ISSN 2306-5249
Online-ISSN 2791-3279
العدد الرابع والعشرون
٢٠٢٤م /١٤٤٦هـ